†Supported by the National Science Foundation.

[1]R. S. Thompson and C.-R. Hu, Phys. Rev. Letters 27, 1352 (1971).

[2]A. Schmid, Physik Kondensierten Materie 5, 302 (1966).

[3]L. P. Gor'kov and G. M. Ėliashberg, Zh. Eksperim. i Teor. Fiz. 54, 612 (1968) [Sov. Phys. JETP 27, 328 (1968)].

[4]G. M. Ėliashberg, Zh. Eksperim. i Teor. Fiz. 55, 2443 (1968) [Sov. Phys. JETP 29, 1298 (1969)].

[5]L. P. Gor'kov and N. B. Kopnin, Zh. Eksperim. i Teor. Fiz. 60, 2331 (1971) [Sov. Phys. JETP 33, 1251 (1971)].

[6]D. Saint-James, E. J. Thomas, and G. Sarma, *Type II Superconductivity* (Pergamon, Oxford, 1969), Chap. 3.

[7]A. A. Abrikosov, Zh. Eksperim. i Teor. Fiz. 32, 1442 (1957) [Sov. Phys. JETP 5, 1174 (1957)].

PHYSICAL REVEIW B VOLUME 6, NUMBER 1 1 JULY 1972

Thermal Effects at Superconducting Point Contacts*

O. Iwanyshyn and H. J. T. Smith
Department of Physics, University of Waterloo, Waterloo, Ontario, Canada
(Received 12 October 1971)

In this paper we have calculated I-V curves of superconducting weak-link constriction junctions by assuming that there is a region of normal material which tends to spread with increasing power levels. The causes for the spreading of the normal resistance are twofold. One is the increase of the current-density distribution and the other is the increase of localized Joule heating at the contact as the total current is increased. The resultant rise in temperature of the link above the bath temperature, over the range of the I-V characteristic, is found to be significant. Using material constants that are representative of bulk Nb, we found that the calculated I-V characteristic is very similar to several experimentally observed Nb point-contact curves. The spreading normal-resistance analysis has suggested a model to explain the I-V characteristic of a superconductor–normal-metal (S–N) point-contact system. A calculation has indicated that large excess temperatures are also present at the contacts when biased in the millivolt region. These findings have prompted us to review several published experiments with S–N contacts.

I. INTRODUCTION

Current-voltage (I-V) characteristics of superconducting weak-link point-contact or thin-film constriction junctions usually exhibit a zero-voltage current followed by either a continuous or discontinuous transition into a nonlinear resistive region.[1-4] The types (Ohmic, flux flow, radiation) of dissipative mechanisms active in this region and the proportions which they contribute to the local resistance are difficult to distinguish in experimental situations.[3,4] It has been well documented in the literature[5] that superconducting phenomena can be present in the resistive state.

In the theory of resistive yet superconducting point contacts at a nonzero voltage the total transport current is generally assumed to consist of a superconducting and a normal component.[6] The superconducting component consists of Cooper pairs and is dissipative because of the emission of photons. The normal component consists of quasiparticles and is also dissipative because of Joule heating. In the simplest approximation such a point contact may be represented[7,8] by an ideal Josephson element, in parallel with a shunt conductance G that exhibits Ohmic behavior.

Several authors[7-9] have calculated the I-V characteristics that result from this model when it is modified by the circuit capacitance and inductance. Scott[10] has found satisfactory agreement between the experimental observation of hysteresis in the I-V characteristics of thin-film Pb-PbO-Pb sandwich junctions and the theoretical predictions of Stewart[7] and McCumber.[8] Although this theory gives good agreement with experiment in the case of some types of weak-link junctions,[11,12] in the case of point-contact junctions poor agreement[13] with experiment is obtained, especially at large biases. This inconsistency may be attributed to an oversimplified picture of the contact model.

To explain their I-V curves with weak-link junctions (both thin-film constrictions and pressure contacts) several authors[1,3] have suggested that the superconducting region adjacent to the contact interface is driven normal by the large current densities localized there, while the surrounding material with lower current density remains superconducting. This process is accompanied by Joule heating at the contact. As current through the contact is increased, the Joule heating and current density in the contact region are increased, resulting in a spread of the region of normal material and hence an increase of the Ohmic resistance. In the models of Stewart and McCumber the shunt con-

ductance G is assumed to be independent of bias voltage. In the model of Scott the shunt conductance G follows the highly nonlinear behavior that is predicted in the theory of superconductor–insulator–superconductor (S–I–S) quasiparticle tunnel junctions.

In the present case we treat the junction as a superconductor–normal-metal–superconductor (S–N–S)-type contact.[13,14] The analysis of the I-V characteristic is complicated for two reasons: (a) The dimensions of the region where dissipation occurs tend to increase as the total current is increased and (b) the temperature of this normal region and the surrounding superconducting material may be several degrees in excess of the bath temperature T_b. At the boundary where the superconductor is in contact with the liquid-helium bath the temperature is assumed to be fixed at T_b. In some experimental situations where this may not be the case excessive heat fluxes can lead to a thermal runaway.[15]

To simplify the calculation of the spread of the normal region we assume that we are working in a region of the I-V characteristic where the pair-current component is much smaller than the normal-current component. Hence the pair-current dissipation due to photons is neglected. Additional dissipative effects due to pair current such as flux flow and phase slippage are also assumed absent. The total current may then be expressed as $I(V) = G(V, d)V$, where d is a constant of the material and the geometry, and the conductance G is the quantity to be calculated as a function of bias voltage for a fixed d. As the bias voltage is increased the normal region increases and so the two superconductors are further decoupled, and thus we expect the calculation to have the most validity at large biases.

The purpose of the following analysis is threefold. Several authors[1,3,4] have indicated that a resistive region as described may be present at a weak link which at the same time exhibits some superconducting properties. It is reasonable to assume that the dimensions of the normal region will influence[3] pair-current phenomena in the resistive state. If the weak links are regarded as simply S–N–S junctions, it is interesting to relate the dimensions of the normal region to each point of the I-V characteristic. We will proceed to do so for the case of two bulk superconductors separated by an electrically insulating layer of negligible thickness, except over a small circular region where they are in direct contact. Second, we wish to comment on the I-V curves observed by Pankove.[16] Finally, our model has indicated that relatively high temperatures can be generated at a point contact when biased in the millivolt region. The implications of such localized excess heating have led us to review several papers in which point contacts were used to pass current from a normal metal to a superconductor.

II. THEORY OF "SPREADING" NORMAL RESISTANCE

A. Case 1: Temperature-Independent Thermal Conductivities

The bulk materials are represented in Fig. 1 as two semi-infinite solids, $z<0$ and $z>0$, that are electrically insulated from one another in the $z=0$ plane except over the region $x^2+y^2\le a^2$, where a defines the constriction radius. The current I through the weak link flows through the constriction region from the upper to the lower bulk regions. When the current I is sufficient to drive the contact region normal, the heat balance in this steady state is described by

$$\sigma(\nabla V)^2 = -\nabla\cdot(k^N\nabla T)\,, \tag{1}$$

where $T(\vec{r})$ is the temperature in the normal material, $k^N(T)$ is the thermal conductivity in the normal material, $\sigma(T)=1/\rho(T)$ is the electrical conductivity in the normal material, and $V(\vec{r})$ is the potential in the normal material, with the additional condition (Kirchoff's law) that

$$\nabla\cdot(\sigma\nabla V)=0\,. \tag{2}$$

With this geometry it is most convenient to adopt the oblate spheroidal coordinate system in which

$$x = a(1+\xi^2)^{1/2}(1-\eta^2)^{1/2}\cos\phi\,,$$

$$y = a(1+\xi^2)^{1/2}(1-\eta^2)^{1/2}\sin\phi\,,$$

$$z = a\xi\eta\,,$$

where

$$-1\le\eta\le1\,,\quad 0\le\xi<\infty\,,\quad 0\le\phi\le2\pi\,.$$

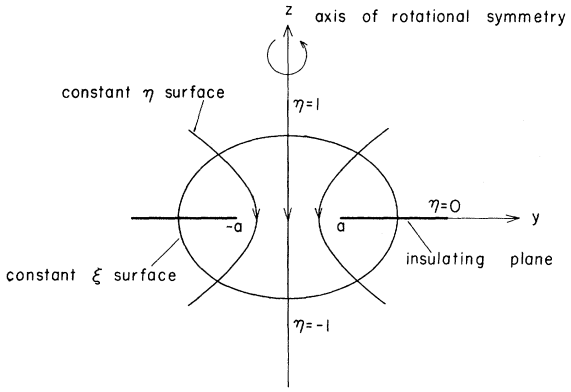

FIG. 1. Oblate spheroidal coordinate system shown in relation to a point contact of radius a. The thick line along the y axis indicates the insulating plane. The paraboloas indicate the strength and direction of current flux, whereas the ellipses represent the equipotentials and isotherms. Rotation about the z axis determines the paraboloid and ellipsoid surfaces.

In this coordinate system, constant ξ and constant $|\eta|$ define ellipsoid and paraboloid surfaces of revolution, respectively, about the z axis, as shown in Fig. 1. The property of isotropy eliminates the dependence on the ϕ coordinate in this analysis.

When a current I flows in a similar geometry of completely normal material, the equipotentials are described in terms of ellipsoid surfaces of revolution[17] with foci a, $-a$. As a first approximation we will assume that the normal-metal–superconductor (N–S) boundary is an ellipsoidal surface defined by $\xi = \xi_0$. Assuming that the equipotential surfaces are also isotherms, it was shown by Kohlrausch[18] that they are related by

$$V^2 = 2\int_T^{T_m} \rho k^N \, dT \,, \tag{3}$$

where T_m defines the maximum temperature obtained at the link. In terms of solving the required differential equations in the normal state, this means that for the case of oblate spheroidal coordinates and the boundary conditions

$$V(\xi_0) = \pm U/2 = IR(\xi_0) \,, \tag{4}$$

where $\pm U/2$ are the potentials at the N–S boundary;

$$T(\xi_0) = T_c \,, \tag{5}$$

where T_c is the temperature at the N–S boundary;

$$T(0) = T_m \,, \quad V(0) = 0 \,, \tag{6}$$

$$\left.\frac{\partial T}{\partial \eta}\right|_{\eta=0} = 0 \quad (\xi < \xi_0). \tag{7}$$

Equations (1) and (2) result in solutions of V and T as functions of ξ only.

The solution to Eq. (2) is then

$$V(\xi) = \frac{\pm U}{2\tan^{-1}\xi_0} \tan^{-1}\xi \,. \tag{8}$$

Assuming constant values for the electrical and thermal conductivities, we use the result[17] that

$$R(\xi_0) = \frac{U}{2I} = \frac{\rho_0}{2\pi a} \tan^{-1}\xi_0 \,, \tag{9}$$

where R is the resistance between the equipotentials $V = 0$ and $V = \pm U/2$. Substitution of Eq. (9) into Eq. (8) leads to

$$V(\xi) = \pm I \frac{\rho_0}{2\pi a} \tan^{-1}\xi \,. \tag{10}$$

The substitution of Eq. (10) into Eq. (3) and integration yield

$$T(\xi) = T_m - \frac{1}{2\rho_0 k_0^N} \left(\frac{I\rho_0}{2\pi a} \tan^{-1}\xi\right)^2 , \tag{11}$$

which from the boundary condition $V(\pm \xi_0) = \pm U/2$ becomes

$$T_m = T_c + \frac{1}{2\rho_0 k_0^N} \left(\frac{I\rho_0 \tan^{-1}\xi_0}{2\pi a}\right)^2 \,. \tag{12}$$

The spatial dependence of the current density in the normal region is obtained from Ohm's law, $J = (1/\rho_0)\nabla V$, which, on substituting Eq. (10), yields

$$J = \frac{I}{2\pi a^2 (\eta^2 + \xi^2)^{1/2} (1 + \xi^2)^{1/2}} \,. \tag{13}$$

Now we turn our attention to the superconducting region. The equation determining the thermal equilibrium in the steady state is

$$\nabla \cdot (k^S \nabla T) = 0 \,, \tag{14}$$

where $k^S(T)$ is the thermal conductivity in the superconducting state. The following boundary conditions must be satisfied:

$$T(\xi \to \infty) = T_b \,,$$

where T_b is the bath temperature,

$$T(\xi_0) = T_c \,,$$

$$\left.\frac{\partial T}{\partial \eta}\right|_{\eta=0} = 0 \qquad (\xi > \xi_0) \,,$$

where, because of symmetry, we assume that no heat travels across the insulator between the two superconductors.

The series solution to Eq. (14) is in terms of spherical-harmonic functions[19] which are reduced by the boundary conditions to the form

$$T(\xi) = T_b + \frac{(T_c - T_b)}{\cot^{-1}\xi_0} \cot^{-1}\xi \,. \tag{15}$$

From the thermal analog of Gauss's law we have

$$\oint_A (k^S \nabla T)_n \, dA = Q \qquad (\xi \geq \xi_0) \,, \tag{16a}$$

where A is a surface enclosing one of the normal regions $z > 0$ or $z < 0$ and Q is a constant equal to the total rate of heat generated in the normal region.

To evaluate Q we note that at the N–S boundary

$$Q = \oint_{A_{\xi_0}} (k^S \nabla T)_n \, dA = \oint_{A_{\xi_0}} (k^N \nabla T)_n \, dA$$

(continuity of heat flux)

$$= \oint_{A_{\xi_0}} \nabla \cdot (k^N \nabla T) \, dV$$

$$= \oint_{V_{\xi_0}} \rho J^2 \, dV = \tfrac{1}{2} IU \,. \tag{16b}$$

Substitution of Eqs. (15) and (9) into (16) and integration yield

$$T_c = T_b + \frac{\rho_0}{k_0^S} \left(\frac{I}{2\pi a}\right)^2 \tan^{-1}\xi_0 \cot^{-1}\xi_0 \,, \tag{17}$$

where we have assumed a constant $k^S = k_0^S$. Equation (17) relates the spread of the normal region to the temperature at the N–S boundary for a fixed I.

A further constraint on T_c is that it must lie be-

low $T_c(0)$, the critical temperature in zero current, and for each such T_c there is associated a critical current density $J_c(T_c)$ above which superconducting material switches into the resistive state. A form of $J_c(T_c)$ has been calculated by Bardeen,[20] where it was assumed that J_c is uniform across the superconductor. This condition is usually satisfied in geometries that have at least one small dimension, e.g., thin films. The relationship is given by

$$\frac{J_c(T_c)}{J_c(0)} = \left[1 - \left(\frac{T_c}{T_c(0)}\right)^2\right]^{3/2} \left[1 + \left(\frac{T_c}{T_c(0)}\right)^2\right]^{1/2}, \quad (18)$$

where $J_c(0) = \frac{1}{2} H_{cb}(0)\,[\Delta(0)/\rho_0\hbar]^{1/2}$ (emu), $J_c(0)$ is the critical current density at $T = 0\,^\circ\mathrm{K}$, $H_{cb}(0)$ is the critical field of bulk material at $T = 0\,^\circ\mathrm{K}$, and $\Delta(0)$ is one-half the energy gap at $T = 0\,^\circ\mathrm{K}$. If we assume that the current density at the N–S interface may be approximated by its distribution in the normal region, then Eq. (13) indicates that the condition of uniform current density is reasonably well satisfied in the present geometry for not too small values of ξ_0.

At this stage our initial approximation that the N–S interface be defined at $\xi = \xi_0$ must be modified since a comparison of Eqs. (13) and (17) indicates that $J_c = J_c(\xi_0, \eta)$ and $T_c = T(\xi_0)$, which is inconsistent with Eq. (18). To overcome this difficulty we assume that the true N–S boundary surface is intermediate to one defined by the temperature $T(\xi_0)$ and the average current density $\bar{J}_c(\xi_0, \eta_0)$, where initially η_0 is set equal to unity. The true normal volume is approximated by taking the average value of the volumes defined by $T(\xi_0)$ and $\bar{J}_c(\xi_0, \eta_0)$. In the latter case a numerical integration was required. It was assumed that the true normal volume is an ellipsoid of the same family as the $T(\xi_0) = T_c$ ellipsoids (i.e., with foci a, $-a$). This calculation results in a new parameter ξ_N which replaces ξ_0 in T_c, T_m, and U; now $\bar{T}_c(\xi_N)$, $\bar{T}_m(\xi_N)$, and $\bar{U}(\xi_N)$ represent the average values of the respective parameters, a consequence of the approximation made at the N–S interface.

The ratios $|[T_c(\xi_0) - \bar{T}_c(\xi_N)]/\bar{T}_c(\xi_N)|$, $|[T_m(\xi_0) - \bar{T}_m(\xi_N)]/\bar{T}_m(\xi_N)|$, and $|[U(\xi_0) - \bar{U}(\xi_N)]/\bar{U}(\xi_N)|$ were calculated to be < 0.05 even for the case when there were pronounced differences in the constant-J_c and the constant-T_c surfaces. The ellipsoid defined by the ξ_N surface is, in addition, subject to the condition that the product of the average value of the current density $\bar{J}_c(\xi_0, \eta_0)$ and the area of the ξ_N surface is equal to I. This defines η_0 at the N–S boundary

The steady-state values for ξ_N, ξ_0, and η_0 were obtained by substituting Eqs. (17) and (14) into (18) and solving numerically the resulting equation for ξ_0. In this initial approximation we set $\eta_0 = 1$. Next ξ_N was calculated, leading to a better value for ξ_0, which was then resubstituted into J_c of Eq. (18), which itself was then re-solved to give a new ξ_0 value. This iterative process was repeated until the differences between succeeding η_0's became negligible. The above procedure was repeated for each current increment to generate the I-V characteristics shown in a normalized form in Fig. 2.

To obtain normalized expressions we set

$$i = \frac{0.1I}{\pi a^2 J_c(0)}\,,$$

$$v = \frac{0.2U}{\pi a J_c(0)\rho_0} = \frac{0.1U}{\pi a^2 J_c(0) R_\infty}\,,$$

where $R_\infty = \rho_0/2a$, $t_m = T_m/T_c(0)$, and $t_c = T_c/T_c(0)$. These expressions are substituted into Eqs. (9), (12), (13), and (17), which then may be rewritten

$$r = \frac{R(\xi_0)}{R_\infty} = \frac{2}{\pi}\tan^{-1}\xi_0\,, \quad (9')$$

$$j_c = \frac{i}{2(1+\xi^2)^{1/2}(\eta^2+\xi^2)^{1/2}}\,, \quad (13')$$

$$t_m = t_c + \delta i^2 (\tan^{-1}\xi_0)^2\,, \quad (12')$$

where

$$\delta = \frac{100[J_c(0)]^2 a^2 \rho_0}{8 k_0^N T_c(0)}$$

and

$$t_c = t_b + \gamma i^2 \tan^{-1}\xi_0 \cot^{-1}\xi_0\,, \quad (17')$$

$$\gamma = \frac{100[J_c(0)]^2 a^2 \rho_0}{4 k_0^S T_c(0)}\,, \quad t_b = \frac{T_b}{T_c(0)}\,.$$

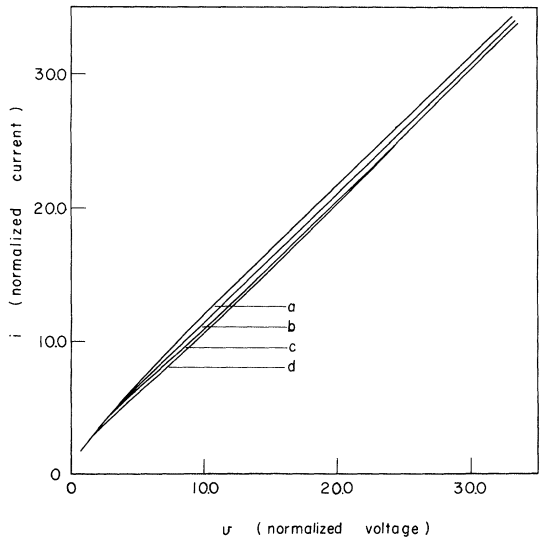

FIG. 2. Normalized i–v curves calculated for several values of (δ, γ), i.e., assuming constant thermal conductivities, and $t_b = 0.47$; (a) $\delta = 0.73 \times 10^{-3}$, $\gamma = 4.4 \times 10^{-3}$; (b) $\delta = 1.65 \times 10^{-3}$, $\gamma = 9.89 \times 10^{-3}$; (c) $\delta = 2.93 \times 10^{-3}$, $\gamma = 17.6 \times 10^{-3}$; and (d) $\delta = 4.58 \times 10^{-3}$, $\gamma = 27.5 \times 10^{-3}$.

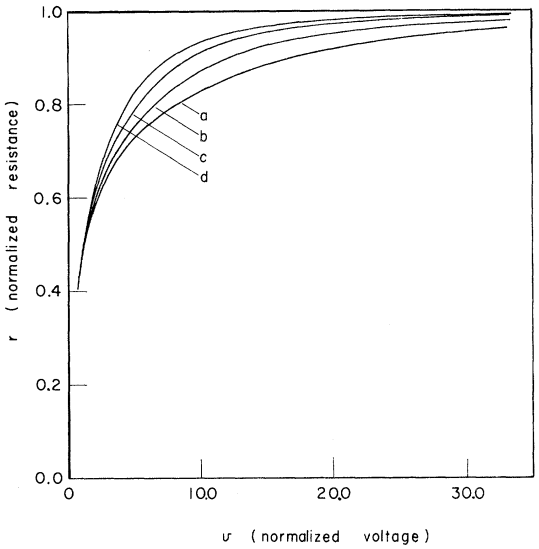

FIG. 3. Dependence of r on v. The values of (δ, γ) for curves (a)–(d) are defined in Fig. 2; $t_b = 0.47$.

In Fig. 3 we show the dependence of r on v. In Figs. 4 and 5 we display $\xi_N(v)$ and $t_m(v)$, respectively.

The unphysical situation of a singularity arising in $J_c(\xi_0, \eta_0)$ as ξ_0 and η_0 both approach zero was not encountered since the solution to the steady-state normal region was not attempted when the J_c surfaces became too distorted [when $(\eta_0^2 + \xi_0^2)(1 + \xi_0^2) < 1$]. At the lowest ξ_N, ξ_0, and η_0 values, when differences between the $\bar{T}_c$ and $\bar{J}_c$ surfaces were most pronounced, J_c varied over the average ξ_N surface by a factor of less than 2.

Results: Case 1

We summarize some of the more interesting features of the generated curves.

In Fig. 2, after an initial nonlinear region $[(d^2v/di^2) > 0]$, the i-v characteristic appears linear and its dynamic resistance is almost equal to the resistance of the i-v characteristic of the same contact when the bulk materials are entirely in the normal state. When this region is extrapolated to $v = 0$, the line passes through a finite current value. From Figs. 3 and 4 we note that $r(v)$ changes very little for $\xi_N > 4$.

The rate of increase of ξ_N with v (Fig. 4) is observed to be slower at low bias voltages than at higher voltages. The slow rate of increase is paralleled by a rapid rise in t_c (Fig. 5). When $t_c \approx$ const, the rate of increase of $\xi_N(v)$ becomes more pronounced. This is to be expected since, if t_c remains almost unchanged with increasing amounts of power dissipated, then the surface at the N–S interface must bear the entire burden of dissipating the increased amounts of heat generated in the region.

Figure 5 indicates that t_c increases with i (since $i \propto v$). Equation (18) implies that there must occur a corresponding decrease in J_c. We conclude that the area of the N–S interface increases faster than i with increasing v.

Finally, the constant-k_0^S, -k_0^N calculation has indicated the presence of large excess temperatures $(t_m \gtrsim 1)$ at the link (Fig. 6). This observation has motivated a refinement in our calculations by in-

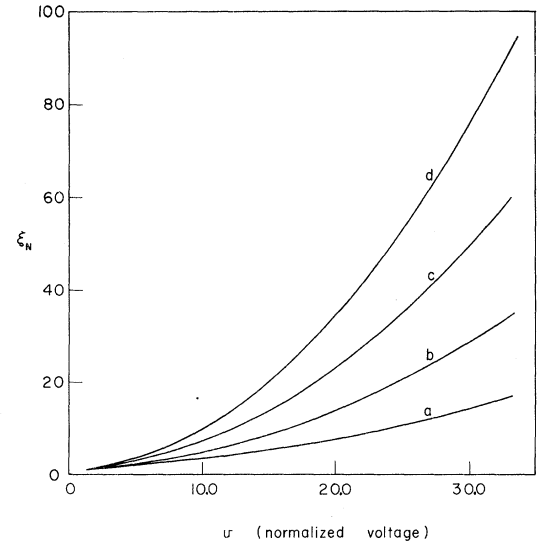

FIG. 4. Dependence of ξ_n on v. The values of (δ, γ) for curves (a)–(d) are defined in Fig. 2; $t_b = 0.47$.

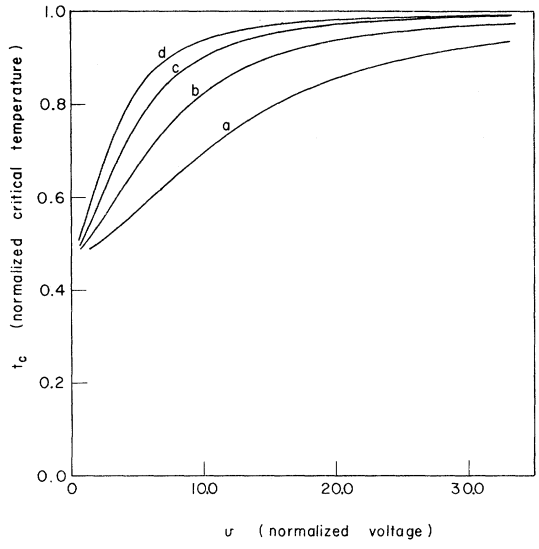

FIG. 5. Dependence of t_c on v. The values of (δ, γ) for curves (a)–(d) are defined in Fig. 2; $t_b = 0.47$.

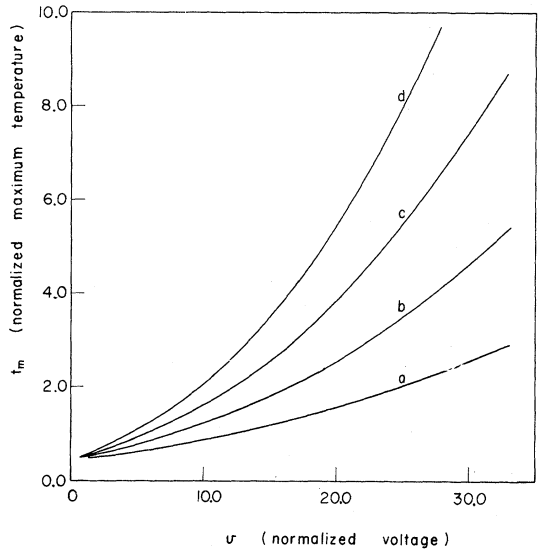

FIG. 6. Dependence of t_m on v. The values of (δ, γ) for curves (a)–(d) are defined in Fig. 2; $t_b = 0.47$.

cluding the temperature dependences of k^S and k^N.

B. Case 2: Temperature-Dependent Thermal Conductivities

The above calculation is repeated and the temperature dependence of the thermal conductivities in both the normal and superconducting regions is included. For metals in the normal state $k^N(T)$ at low temperatures may be written[21]

$$k^N(T) = \frac{1}{\alpha T^2 + \beta/T} \ , \tag{19}$$

where α and β are material constants. In the superconducting state[22]

$$k^S(T) = k^N(T)\,\frac{2F_1(-y) + 2y\ln(1+e^{-y}) + y^2/(1+e^{y})}{2F_1(0)} \ , \tag{20}$$

where $y = \Delta(T)/kT$, k is Boltzmann's constant, $2\Delta(T)$ is the temperature-dependent energy gap, and $F_1(y)$ is the Fermi-Dirac function and is tabulated in Ref. 23. In the numerical computations the right-hand side of the above equation was approximated by a third-order polynomial to within 1% of its true values. $\Delta(T)$ was assumed to follow the BCS behavior.[24] To obtain an explicit expression for T_m we used Eq. (16:09) in Ref. 17,

$$\frac{R_{\xi_0}(\rho_0, k_0^N)}{R_{\xi_0}(\rho, k^N(T))} = \frac{1}{V(\rho, k^N(T))}\int_{T_c}^{T_m} \frac{\rho_0 k^N(T)\,dT}{\left[2\int_T^{T_m} \rho k^N(T)\,dT\right]^{1/2}} \tag{21}$$

and approximated Eq. (19) by

$$k^N(T) = \frac{L_0}{\rho_0}\,T \quad (T \le T_0) \quad \text{(Wiedemann-Franz law)}$$

$$= \frac{L_0 T_0}{\rho_0} \quad (T > T_0) \ , \tag{22}$$

where L_0, the Lorenz number, is equal to $2.45 \times 10^{-8}\ \mathrm{W\,\Omega/^\circ K^2}$. As before, we assume $\rho \approx \rho_0$. This leads to the following expression for T_m:

$$T_m = \left(\frac{[IR_{\xi_0}(\rho_0, k_0^N)]^2}{L_0} + T_c^2\right)^{1/2} \quad (T_m \le T_0) \tag{23a}$$

$$= \frac{[IR_{\xi_0}(\rho_0, k_0^N)]^2 + L_0T_0^2 + L_0T_c^2}{2L_0T_0} \quad (T_m > T_0) \ . \tag{23b}$$

The approximate expression for U is obtained from the Kohlrausch relation [Eq. (3)] and Eq. (22). Integration yields

$$U = 2[L_0(T_m^2 - T_c^2)]^{1/2} \quad (T_m \le T_0) \tag{24a}$$

$$= 2[2L_0T_0(T_m - T_0) + L(T_0^2 - T_c^2)]^{1/2} \quad (T_m > T_0) \ . \tag{24b}$$

In order to obtain an expression for ξ_0 we assume that the surfaces of constant temperature remain ellipsoids; i.e., the temperature is a function of ξ only. Equations (16) then lead to the relation

$$\int_{T_c}^{T_b} k^S(T)\,dT = -\frac{IU}{4\pi a}\cot^{-1}\xi_0 \ . \tag{25}$$

The approximation to Eq. (20) by a third-order polynomial implies that the left-hand side of Eq. (25) may be simply integrated to obtain

$$\xi_0 = \cot(4\pi a/IU)(C_4T_c^4 + C_3T_c^3 + C_2T_c^2 + C_1T_c + C_0) \ , \tag{26}$$

where C_4, C_3, C_2, C_1, and C_0 are constants. Once ξ_0 has been evaluated, T_c can be obtained from Eq. (18).

Starting with an initial value for T_c and $\eta = \eta_0$ as before, Eqs. (23), (24), (26), and (18) are solved self-consistently. As in the previous calculation, the conditions requiring that the true volume of normal material is intermediate to the volumes defined by the constant-$\bar{J}_c$ and constant-T_c surfaces and that $\bar{J}_c(\xi_0, \eta_0) \times (\text{area of } N\text{–}S \text{ interface}) = I$ determines the values of the parameters ξ_N and η_0, respectively.

To calculate the normal-state I-V curve (both of the semi-infinite slabs are in the normal state), T_c in Eqs. (21) and (24) is replaced by T_b, and R_{ξ_0} in Eq. (21) is set equal to $\rho_0/4a$.

Results: Case 2

The essential features of the curves obtained by setting $k^N = k_0^N$ and $k^S = k_0^S$ are retained in the $k^N(T)$, $k^S(T)$ calculations. For ease of comparison with actual experimental curves we have used values of material properties that are representative of bulk Nb. An I-V characteristic calculated using $\rho_0 = 1.35 \times 10^{-6}\ \Omega\,\mathrm{cm}$ and $a = 58$ Å is shown in Fig. 7. In relation to the I-V curves it was found that at low-bias voltages the region exhibiting large curvature changes, $d^2V/dI^2 > 0$, is compressed closer towards the origin. As in the constant-k_0^S, -k_0^N calculation,

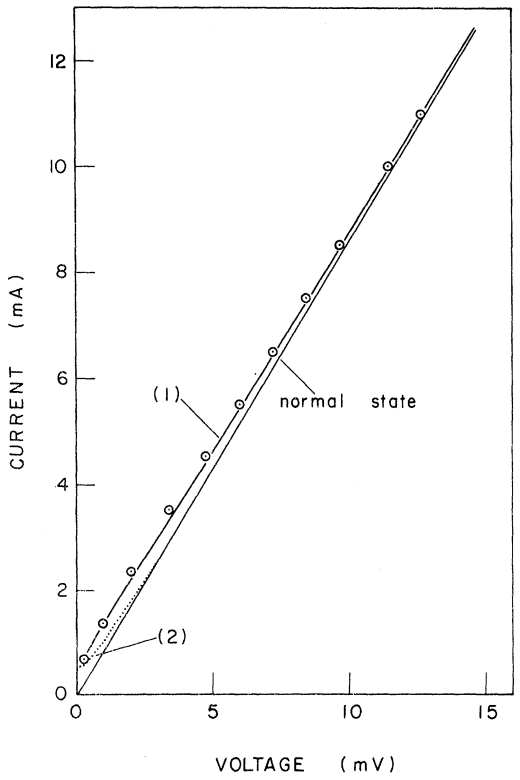

FIG. 7. Curve (1) refers to the I-V characteristic determined by the spreading resistance model for the case case of a Nb point contact ($a = 58$ Å, $T_b = 4.2$ °K) where the temperature dependence of the thermal conductivities is included. The circled points are obtained from Pankove's curve [Ref. 16, Fig. 1 (a)]. Curve 2 is obtained from Eq. (30), in which we set $R = 1/G = 1.17$ Ω and $i_m = 0.5$ mA. The normal-state curve is common to all three curves.

an increase in the residual resistivity ρ_0 increases the magnitude of d^2V/dI^2. For the case of Nb the approximation for $k^N(T)$ places an upper limit[21] $T_m \sim 60$ °K for which the I-V curve may be calculated. In Fig. 8 we have plotted $\Delta T = T_m - T_b$ against V as calculated from our model. We compare this curve to the one obtained from the Kohlrausch relation with T_c being approximated by T_b. Note that at small bias voltages the differences between the two curves are approximately 2 °K.

III. REEXAMINATION OF CERTAIN EXPERIMENTAL DATA

A. Superconductor-Superconductor Point Contacts

From an analysis of the I-V characteristic of point contacts at crossed Nb wires Pankove[16] concluded that at large bias voltages ($eV > 2\Delta$) a fraction of the total current is superconducting. The presence of this supercurrent was associated with the realization of a superconducting state at the contact due to the large current densities ($\sim 10^9$ A/cm^2) arising at the constriction. In this region Pankove proposed a contact model wherein part of the total current passed through a resistive-tunneling component and the rest through a saturable but *not* current-quenchable superconducting component. The possibility of high-current superconductivity has been theoretically explored by Parmenter.[25]

A comparison of Pankove's experimental results for a Nb crossed-wire junction with the theoretical curves obtained from the analysis of Sec. II B (Fig. 7) shows that they are very similar. The material constants were those of bulk niobium with $a = 58$ Å for $R_\infty = 1.17$ Ω (cf. $a = 25$ Å for $R_\infty = 1.17$ Ω calculated by Pankove[16]). The differences between the two curves may result from an error in the estimate of the residual resistivity ρ_0, which was taken from Ref. 21. A larger yet physically acceptable ρ_0, as might be expected in the contact region, would considerably reduce these differences. However, in view of the approximations involved—in particular, the differences in geometry—the reasonable agreement evidenced in Fig. 7 was felt to be satisfactory. Hence it may be concluded that the model proposed by Pankove is not necessary to explain the I-V characteristic. The curve may be regarded as being characteristic of a localized-heating phenomenon occurring at superconducting point contacts in the resistive state. Furthermore, the absence of a sudden rise in quasiparticle current at the energy gap suggests that the component of the total current due to tunneling is negligible, as assumed in our

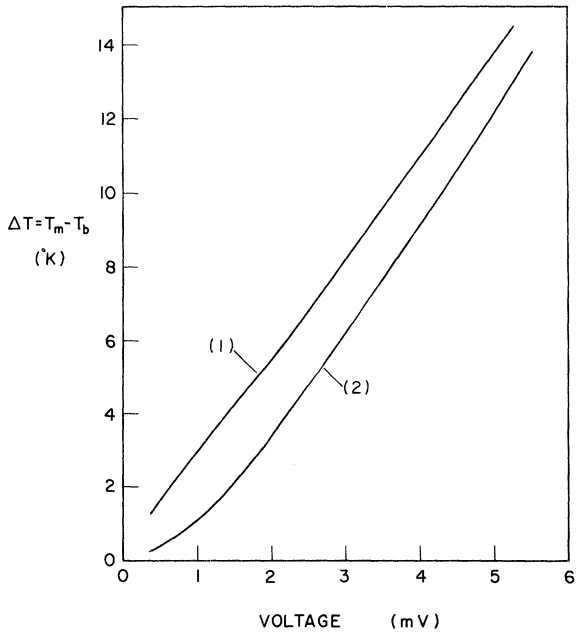

FIG. 8. Curve (1) refers to $T_m(V)$ that was calculated in the derivation of curve (1) of Fig. 7. Curve (2) is obtained assuming that the N–S boundary is located at $\xi = \infty$.

theoretical analysis. These conclusions are further corroborated by Barnes,[26] who, in his published I-V curves of Nb point-contact junctions, illustrates those curves which exhibit the sudden increase of quasiparticle current at $eV = 2\Delta$ and those which do not, but, in the latter case, bear a close similarity to our generated curve. A general difference between the two types of curves is that the current magnitudes are of the order of μA in the former and mA in the latter.

B. Superconductor-Normal-Metal Point Contacts

Investigations of the electrical characteristics of point contacts between bulk samples of superconducting and normal materials have been reported in the literature.[16,27–30] I-V characteristics of such junctions are generally of the form shown in the schematic representation of Fig. 9(a). Assuming a multicontact junction, the equivalent resistive circuit from which this curve could be obtained is shown in Fig. 9(b). The symbols R_{D1}, R_{D2}, ... represent the resistances in the bulk material that result from the configuration of current and potential probes and may take on different values when the locations of these probes are changed. The symbols R_{C1}, R_{C2}, ... represent the constriction resistances in the normal material at each point contact. It is usually the case that R_{D1}, R_{D2}, ... $\ll R_{C1}$, R_{C2}, ... The resistive units R_{S1}, R_{S2}, ... within the dashed rectangle behave as described in Sec. II. Below the critical currents $I_{c1}(\uparrow)$, $I_{c2}(\uparrow)$, ... the resistances R_{S1}, R_{S2}, ... are all equal to zero.

The I-V characteristic is determined in the following manner. The initial Ohmic region is due to the constriction resistances in the normal material. At larger currents the I-V characteristic begins to deviate from its linear form $[(d^2V/dI^2) > 0]$. This effect may be connected with an increase of generated Joule heating in the normal material localized at the contacts which raises the temperature in the adjacent superconducting regions and in some cases drives the narrowest constrictions normal in the manner previously described. With further current increases the number of such occurrences increases, until at I_c a near-simultaneous cumulative chain-reaction-like process results in all the links switching normal. Past the instability an increase of current results in the localized spreading of the normal regions in the superconducting material. As shown in Sec. III A, the relation between current and voltage in this region is approximately linear such that when it is extrapolated to zero voltage it intersects the current axis at a positive finite value. The quantitative description of the above process is quite complex and has not been attempted.

Fournet and Milleron,[28] to explain such a characteristic, proposed a model whereby the N-S interface contained constrictions that could be separated into two classes: those that weitched normal at I_c and those that remained superconducting until the bulk material switched normal. This somewhat artificial distinction of constriction sizes is superfluous in terms of our model involving a spreading resistance beyond I_c. We mention in passing that the I-V characteristic of the contact between crossed normal and superconducting wires observed by Pankove[16] can also be explained by this model.

If we consider that the thermal conductivity of the normal material is much greater than that of the superconducting material and if the effect of preliminary switching is taken into account, we obtain the quantity V_1 [Fig. 9(a)], which can be regarded as the potential difference across the point contacts (at I_c) in the normal material. Assuming that most of the heat generated at the contacts is transferred by the normal material, we can calculate, by means of the Kohlrausch relationship, the excess temperature at the contacts:

$$V_1^2 = 2\int_{T_b}^{T_m} \rho k^N dT \,. \tag{27}$$

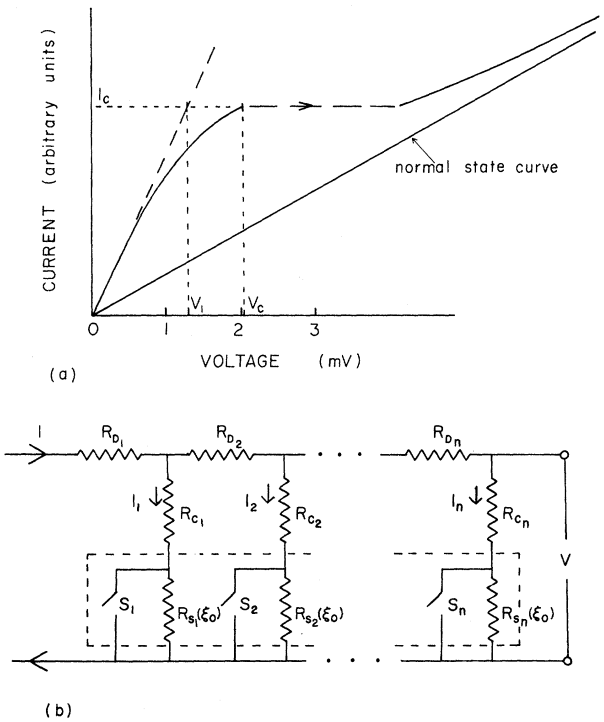

FIG. 9. (a) Schematic I-V characteristic commonly observed with S–N point-contact junctions. (b) The equivalent circuit from which the I-V characteristic of Fig. 9(a) may be obtained. Note that for I_1, I_2, ... $< I_{c1}$, I_{c2}, ... switch S_1, S_2, ... is closed.

For the case of copper as the normal metal and T_m not too large ($\lesssim 15\,^\circ$K) we may set[21] $\rho \cong \rho_0$ and $k^N = (L_0/\rho_0)T$ and, on substituting into Eq. (27), obtain

$$T_m = (T_b^2 + V_1/L_0)^{1/2} . \tag{28}$$

The above analysis has been applied to the reported I-V characteristics of Sullivan and Roos,[29] who postulated a novel switching mechanism occurring at $V = V_c$ (as defined in Fig. 9). This mechanism assumed that at V_c the bath temperature was maintained uniformly throughout the junction. The scatter in their experimental results was attributed solely to proximity effects at the N–S boundary. At $V = V_1$ and $T_b = 2.16\,^\circ$K we have calculated that the excess temperature ($\Delta T = T_m - T_b$) is ~ 4–$5\,^\circ$K. In our model ΔT is independent of the specific form of the critical parameter that, when exceeded, gives rise to the switching instability. It is quite likely that the large discrepancies reported in Ref. 29 between experimental and theoretical values of $V_c(0)/kT_c$ may be substantially reduced if a temperature correction, as indicated by Eq. (28), is applied. Furthermore, in regard to their observations that good normal-metal conductors resulted in a well-defined voltage break, our model, which is based on purely thermal effects, indicates that good thermal and electrical conductivities produce relatively less excess heating and at the same time dissipate this heat more readily. This would allow for relatively larger supercurrents at $V < V_c$ than if the junction were made of a poorly conducting metal. Hence a large I_c would occasion a correspondingly large voltage jump across the region of instability as the size of the normal regions in the superconducting material would have to adjust to the steady-state equilibrium conditions as described previously in Sec. II. Qualitatively similar behavior would be expected if a superconductor with poor electrical and thermal conductivities was substituted for a superconductor with good ones. This was also observed by Sullivan and Roos. The low value of the energy gap for Nb_3Sn reported by Seidel and Wicklund[30] may well be due to localized heating in the oxide region. Their I-V curves (Fig. 1 of Ref. 30) are indicative of an excess current due to pinholes.

IV. DISCUSSION OF RESULTS

Our analysis explains only a limited region of the I-V characteristic of point contacts. We now examine the limitations of our model in the more general context of the theories of Stewart and McCumber.

As indicated in Ref. 14, the behavior of the pair current can be described by a Josephson-type parametric element in which the current is a sinusoidal function (periodic in any case) of the phase difference between the two superconductors. According to our model the effect of the quasiparticle current is represented by a conductance G in parallel with the Josephson element. In this model we have shown that G depends on V and so differs from most previous formulations of the weak-link contact. Symbolically the total current is represented as

$$I(t) = i_q(t) + i_p(t) ,$$

where

$$i_p(t) = i_m(G)\sin\Theta(t) .$$

$\Theta(t)$ is the phase difference of the wave functions on the two sides of the barrier; i_m is the pair-tunnel current maximum and is dependent on junction material, geometry, temperature, and G; and

$$i_q(t) = G[V(t), d]\,V(t) .$$

It is assumed that the bias voltage measured across G is given by $V(t) = (\hbar/2e)\dot{\Theta}(t)$. In the most common experimental situation the junction is driven by a constant current source. Under such conditions one must take into account the capacitance between the two superconductors. The equation describing such a system is

$$I = C(G)\frac{dV(t)}{dt} + G[V(t), d]\,V(t) + i_m(G)\sin\Theta(t) . \tag{29}$$

For the ideal case of $C \to 0$ and G a constant[7,8]

$$\overline{V} = (1/G)(I^2 - i_m^2)^{1/2} , \tag{30}$$

where the bar over a symbol indicates the time average.

For the sake of comparison we have displayed in Fig. 7 the I-V characteristic determined by Eq. (30) where $G = 1/R_\infty$ and i_m are experimental values obtained from Fig. 1(a) of Ref. 15. For a nonzero C and finite G the solution to Eq. (29) has been obtained numerically and the resulting I-V characteristic exhibits hysteresis. For any value of C in the limit of large V, $\overline{V} = I/G$, and as $C \to \infty$, $\overline{V} = I/G$ for any $\overline{V} > 0$.

However, when G is not constant but is a function of V, one would expect C and i_m to vary in a complicated manner. A coarse estimate indicates that the capacitive effect due to the spreading normal region is several orders of magnitude smaller than that arising from junction geometry (10^{-10}–10^{-12} F) and that i_m decreases exponentially[31] with the spread of the normal region. The simultaneous increase of the temperature of the link above T_b due to the Joule heating results in $i_m = 0$ when $T_m \gtrsim T_c(0)$. Furthermore, as V is increased the frequency of the ac current increases until the junction sees a constant voltage when the capacitive admittance ωC dominates the conductance. All these effects tend to limit the region of applicability of Eq. (29) in comparison to the constant G, C, and i_m case.

Therefore, except for small bias voltages ($V < \hbar G/2eC$), the I-V characteristic may be approximated by

$$\bar{V} = V = I/\bar{G}(V, d) \quad .$$

For the case of a circuit driven by a constant voltage source the oscillating pair current averages out to zero, i.e., neglecting inductive effects, and

$$\bar{I} = G(V, d)V \ .$$

These results are consistent with our original simplification, which assumes that, except at very small bias voltages, the form of the I-V characteristic will be mainly influenced by the behavior of $G(V, d)$.

For small voltages the thermal and ac Josephson effects may be present simultaneously, indicating that Eq. (29) should be solved in conjunction with the thermal-effect analysis given in this paper. At even smaller voltages the thermal effects become negligible. Published[13,32] I-V characteristics of constriction contacts suggest that the thermal and ac Josephson effects may exist simultaneously. Additional effects would arise near $T_c(0)$ (or $H \sim H_c$) when it would become energetically favorable for dissipation resulting from flux flow, fluctuations, etc.

Although the approximation in our calculation place a lower limit on $G(V)$, on the basis of qualitative physical arguments we would expect the I-V characteristic to exhibit thermal hysteresis due to the temperature dependence of the critical current density at the contact. Another possible source of hysteresis is usually associated with the dominance of circuit inductance or flux-flow phenomena in determining the I-V characteristic.

The presence of a very thin oxide film in the constriction interface (S–I–S) would result in a large increase of the contact resistance. Hence for constant power dissipation the current must be much smaller [for $eV \cong 2\Delta$, $I^2R(S\text{–}S) \gg I^2R(S\text{–}I\text{–}S)$]. Although the excess temperature in the S–I–S junction would be smaller than for the S–S junction, the temperature rise in the region of the contact could result in the observation of excess current[33] in the region of the energy gap and a reduced value[34] for the energy gap in the I-V characteristic.

Other mechanisms resulting in I-V characteristics that at large bias voltages are similar to the calculated curves have been proposed. From a model involving flux motion the superconducting I-V characteristic of large [λ_J/(junction width) $\ll 1$, where λ_J is the Josephson penetration depth] S–N–S junctions has been calculated and observed experimentally by Waldram *et al.*[12] It was shown that the asymptote of the characteristic when extrapolated to zero voltage intercepted the current axis at a positive finite value, as observed with our model. A similar characteristic has been observed[35] using the "Notarys-bridge" weak-link device. Neither of the above examples involve constriction-type devices, e.g., point contact or Dayem bridge, where small power inputs may result in very high heat fluxes and where the application of the flux-flow model to the small constriction dimensions is not clear. At present we are not aware of a quantitative description of flux-flow dissipation that applies to point contacts.

V. SUMMARY

(i) The S–S point-contact I-V characteristic resulting from a spreading resistance model in the region of the characteristic where $I = \bar{i}_q$ has been calculated.

(ii) The model has indicated the possibility of large excess temperatures localized at the contact.

(iii) The calculated I-V curves have been found to be in satisfactory agreement with curves observed experimentally by others.

(iv) On the basis of this model we proposed a qualitative description of S–N point-contact junctions. A calculation has indicated that a highly conducting normal metal such as copper cannot ensure $T = T_b$ at the link, as assumed in many experiments.

(v) The presence of patchy uneven oxide surfaces has often been linked with anomalous resistive behavior in tunneling characteristics. An explanation in terms of a Joule heating mechanism should not be discounted.

---

*Work supported in part by the National Research Council of Canada.

[1]J. E. Zimmerman and A. H. Silver, Phys. Rev. 141, 367 (1966).

[2]R. DeBruyn Ouboter, M. H. Omar, A. J. P. T. Arnold, T. Guinau, and K. W. Taconis, Physica 32, 1448 (1966).

[3]A. F. G. Wyatt, in *Tunneling Phenomena in Solids*, edited by E. Burstein and S. Lundqvist (Plenum, New York, 1969), p. 541; A. F. G. Wyatt, V. M. Dmitriev, and W. S. Moore, in *Proceedings of the Tenth International Conference on Low-Temperature Physics*, 1966, edited by M. P. Malkov (Viniti, Moscow, 1967), Vol. III A, p. 242.

[4]I. M. Dmitrenko, A. A. Shablo, and L. E. Kolinko, in *Proceedings of the Tenth International Conference on Low-Temperature Physics*, 1966, edited by M. P. Malkov (Viniti, Moscow, 1967), Vol. II A, p. 355.

[5]For a review of superconductive tunneling phenomena, see B. N. Taylor, J. Appl. Phys. 39, 2490 (1968).

[6]J. Bardeen and J. R. Schrieffer, in *Progress in Low Temperature Physics III*, edited by C. J. Gorter (North-Holland, Amsterdam, 1961), p. 170.

[7]W. C. Stewart, Appl. Phys. Letters 12, 277 (1968).

[8]D. E. McCumber, J. Appl. Phys. 39, 3113 (1968).
[9]L. G. Aslamazov and A. I. Larkin, Zh. Eksperim. i Teor. Fiz. Pis'ma v Redaktsiya 9, 150 (1969) [Sov. Phys. JETP Letters 9, 87 (1969)].
[10]W. C. Scott, Appl. Phys. Letters 17, 166 (1970).
[11]P. K. Hansma, G. I. Rochlin, and J. N. Sweet, Phys. Rev. B 4, 3003 (1971).
[12]J. R. Waldram, A. B. Pippard, and J. Clarke, Phil. Trans. Roy. Soc. London A268, 265 (1970).
[13]I. M. Dmitrenko, S. I. Bondarenko, and T. P. Narbut Zh. Eksperim. i Teor. Fiz. 57, 1513 (1969) [Sov. Phys. JETP 30, 817 (1970)].
[14]D. E. McCumber, J. Appl. Phys. 39, 2503 (1968).
[15]R. F. Broom and E. H. Rhoderick, Brit. J. Appl. Phys. 11, 292 (1960); W. H. Cherry and J. I. Gittleman, Solid-State Electron. 1, 287 (1960); J. M. Bremer and V. L. Newhouse, Phys. Rev. Letters 1, 282 (1958).
[16]J. I. Pankove, Phys. Letters 21, 406 (1966); in *Proceedings of the Tenth International Conference on Low-Temperature Physics*, 1966, edited by M. P. Malkov (Viniti, Moscow, 1967), Vol. IIA, p. 257.
[17]R. Holm, *Electric Contacts* (Springer-Verlag, Berlin, 1967), pp. 14–17, 71–74.
[18]F. Kohlrausch, Ann. Physik Leipzig 1, 132 (1900).
[19]W. R. Smythe, *Static and Dynamic Electricity* (McGraw-Hill, New York, 1950), pp. 160–161.
[20]J. Bardeen, Rev. Mod. Phys. 34, 667 (1962).
[21]H. M. Rosenberg, Phil. Trans. Roy. Soc. London A247, 441 (1955).
[22]J. Bardeen, G. Rickayzen, and L. Tewordt, Phys. Rev. 113, 982 (1959).
[23]P. Rhodes, Proc. Roy. Soc. (London) A204, 396 (1950).
[24]G. Rickayzen, *Theory of Superconductivity* (Wiley, New York, 1965).
[25]R. H. Parmenter, Phys. Rev. 116, 1390 (1959); 140, A1952 (1965).
[26]L. J. Barnes, Phys. Rev. 184, 434 (1969).
[27]F. Bedard and H. Meissner, Phys. Rev. 101, 26 (1956).
[28]G. Fournet and P. F. Milleron, Phys. Letters 22, 398 (1966).
[29]D. B. Sullivan and C. E. Roos, Phys. Rev. Letters 18, 212 (1967).
[30]T. Seidel and A. W. Wicklund, in *Proceedings of the Eighth International Conference on Low-Temperature Physics*, edited by R. O. Davies (Butterworths, London, 1963), p. 176.
[31]J. Clarke, Rev. Phys. Appl. 5, 32 (1970); Proc. Roy. Soc. (London) A308, 447 (1969).
[32]J. E. Mercereau, Rev. Phys. Appl. 5, 13 (1970).
[33]J. E. Nordman and W. H. Keller, Phys. Letters 36A, 52 (1971).
[34]Y. Goldstein, Rev. Mod. Phys. 36, 213 (1964); R. W. Cohen, G. D. Cody, and Y. Goldstein, RCA Rev. 25, 433 (1964).
[35]R. K. Kirschman, H. A. Notarys, and J. E. Mercereau, Phys. Letters 34A, 209 (1971).

PHYSICAL REVIEW B VOLUME 6, NUMBER 1 1 JULY 1972

Nonlinear Properties of Fluxoids in Superconductors in a High-Speed Flux-Flow State

Masanori Sugahara
Faculty of Engineering, Yokohama National University, Ohoka, Yokohama, Japan
(Received 17 May 1971)

The order-parameter variation and the electric current about the normal core of a fluxoid in high-speed motion in clean superconductors in the low-magnetic-field and low-temperature region are discussed on the basis of a time-dependent Ginzburg-Landau equation and a classical equation of motion for the core electrons. It is found that the normal current flow along the core electric field tends to a constant when the fluxoid velocity exceeds $(\xi_0/\tau)(1+\omega_c^2\tau^2)$, where ξ_0 is the coherence length, τ is the transport relaxation time, and ω_c is the cyclotron frequency. Expressions of the strain field associated with high-speed fluxoids are derived by the use of a modified elastic-wave equation with superconductivity parameters and are used to investigate the fluxoid velocity dependence of the flux-pinning effect. It is shown that the supersonically accelerated fluxoids radiate elastic shock wave, and that flux pinning by internal strain sources like dislocations is expected to disappear. A wave radiation and lowering of the pinning are also found when fluxoids are subjected to a high-frequency vibration.

I. INTRODUCTION

There have been a number of experiments[1] associated with the motion of fluxoids in the mixed state of type-II superconductors. The flux-flow phenomena have been theoretically treated in semiphenomenological ways[2–8] or with the help of time-dependent Ginzburg-Landau (TDGL) equations.[9–11] However, the fluxoid motion in the low-temperature ($T \sim 0$ °K) and the low-field ($H \gtrsim H_{c1}$) region has only been dealt with semiphenomenologically and for slowly moving fluxoids (the distance a fluxoid moves in the electron relaxation time τ is much smaller with the core radius of fluxoids). Most of the semiphenomenological theories investigate the mixed state using a two-fluid model and hydrodynamic assumptions. The approach cannot describe consistently the properties of fluxoids in high-speed motion. In Sec. II we consider the variation of the order parameter around the core